

CTEQ-805

MSUHEP-80501

UR-1539

January 7, 2018

 **$k_T$  Effects in Direct-Photon Production**

L. Apanasevich, C. Balázs, C. Bromberg, J. Huston, A. Maul, W. K. Tung

*Department of Physics and Astronomy, Michigan State University, East Lansing, MI 48824, USA*

S. Kuhlmann

*High Energy Physics Divison, Argonne National Laboratory, Argonne, IL 60439, USA*

J. Owens

*High Energy Physics, Florida State University, Tallahassee, FL 32306, USA*

M. Begel, T. Ferbel, G. Ginther, P. Slattery, M. Zieliński

*Department of Physics and Astronomy, University of Rochester, Rochester, NY 14627, USA*

We discuss the phenomenology of initial-state parton- $k_T$  broadening in direct-photon production and related processes in hadron collisions. After a brief summary of the theoretical basis for a Gaussian-smearing approach, we present a systematic study of recent results on fixed-target and collider direct-photon production, using complementary data on diphoton and pion production to provide empirical guidance on the required amount of  $k_T$  broadening. This approach provides a consistent description of the observed pattern of deviation of next-to-leading order QCD calculations relative to the direct-photon data, and accounts for the shape and normalization difference between fixed-order perturbative calculations and the data. We also discuss the uncertainties in this phenomenological approach, the implications of these results on the extraction of the gluon distribution of the nucleon, and the comparison of our findings to recent related work.

## INTRODUCTION

Direct-photon production has long been viewed as an ideal vehicle for measuring the gluon distribution in the proton [1]. The quark-gluon Compton scattering subprocess ( $gq \rightarrow \gamma q$ ) dominates  $\gamma$  production in all kinematic regions of  $pp$  scattering, as well as for low to moderate values of parton-momentum fraction,  $x$ , in  $\bar{p}p$  scattering; the cross sections have been calculated to next-to-leading order (NLO) [2]. The gluon distribution in the proton is relatively well-constrained at small  $x$  ( $x < 0.1$ ) by deep-inelastic scattering (DIS) and Drell-Yan (DY) data, but less so at larger  $x$  [3]. Consequently, direct-photon data from fixed-target experiments that have been incorporated in several modern global parton distribution function analyses can, in principle, provide a major constraint on the gluon content at moderate to large  $x$  [4–7].

However, a pattern of deviations between the measured direct-photon cross sections and NLO calculations has been observed [8]. The discrepancy is particularly striking in the recently published higher-statistics data from E706 experiment [9]. E706 observed large deviations between NLO calculations and data, for both direct-photon and  $\pi^0$  inclusive cross sections. The final direct-photon results from UA6 [10] also exhibit evidence of similar, although smaller, discrepancies. The suspected origin of the disagreements is from effects of initial-state soft-gluon radiation. Such radiation generates transverse components of initial-state parton momenta, referred to in this discussion as  $k_T$ . To be precise, as in [9],  $k_T$  denotes the magnitude of the effective transverse momentum vector,  $\vec{k}_T$ , of each of the two colliding partons.

Evidence of significant  $k_T$  has long been observed in measurements of dimuon, diphoton, and dijet pairs. A collection of measurements of the average transverse momentum of the pairs ( $\langle p_T \rangle_{pair}$ ) is presented in Fig. 1, for a wide range of center-of-mass energies ( $\sqrt{s}$ ) [11].

The values of  $\langle p_T \rangle_{pair}$  are large, and they increase approximately logarithmically with increasing  $\sqrt{s}$ . The values of  $\langle k_T \rangle$  per parton (estimated as  $\approx \langle p_T \rangle_{pair} / \sqrt{2}$ ) indicated by these DY, diphoton, and dijet data, as well as the inclusive direct-photon and  $\pi^0$  production

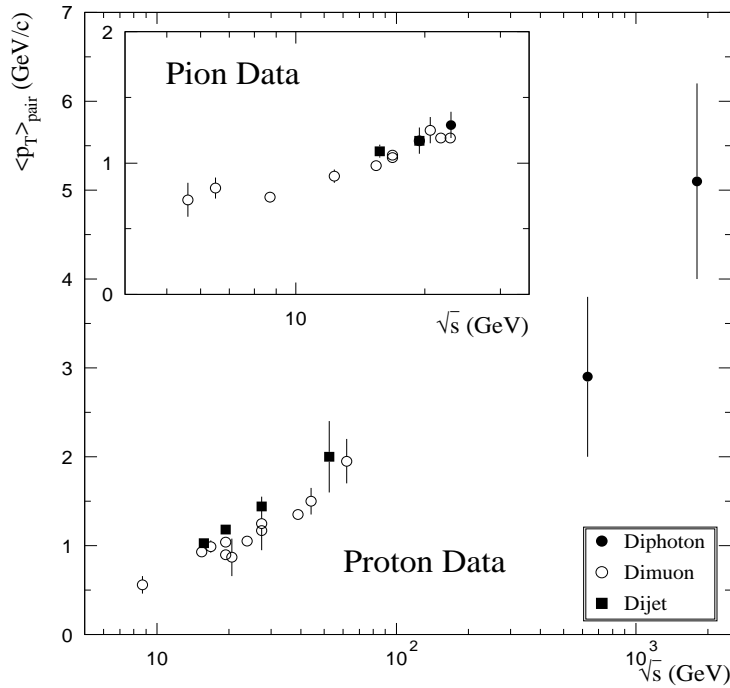


FIG. 1.  $\langle p_T \rangle$  of pairs of muons, photons, and jets produced in hadronic collisions versus  $\sqrt{s}$ .

data, are too large to be interpreted as “intrinsic” — i.e., due only to the finite size of the proton. (From these data, one can infer that the average  $k_T$  per parton is about 1 GeV/ $c$  at fixed-target energies, increasing to 3–4 GeV/ $c$  at the Tevatron collider. One would expect  $\langle k_T \rangle$  values on the order of 0.3–0.5 GeV/ $c$  based solely on proton size.) Perturbative QCD (PQCD) corrections at NLO level are also insufficient to explain the size of the observed effects, and full resummation calculations are required to describe DY and W/Z [12–14], and diphoton [15,16] distributions. Values of  $\langle p_T \rangle_{pair}$  for DY and diphoton data exhibit similar trends versus energy; for DY data, pion-beam values are somewhat larger than those for proton beams at the same  $\sqrt{s}$ . The dijet data hint at somewhat larger values of  $\langle p_T \rangle_{pair}$  than DY results at the same energy, a difference that may be related to different color-flow between initial and final states in DY and in dijet events, as well as to a larger contribution from gluon-induced subprocesses for dijet production. Similar soft-gluon (or  $k_T$ ) effects are expected to be present in all hard-scattering processes, such as the inclusive production of

jets or direct photons [17].

This paper presents a phenomenological model for  $k_T$  effects in direct-photon production and, by extension, in all hard-scattering processes. Quantitative comparisons of this model with data from E706 have been reported previously [9,18]. We will discuss the successes and uncertainties of this prescription, as well as the implications for determining the gluon distribution.

### $k_T$ SMEARING FORMALISM: THEORY AND PRACTICE

We now briefly describe the theoretical underpinnings of  $k_T$  effects using the Collins-Soper-Sterman (CSS) formalism [19]. In this formalism, the  $p_T$  spectrum in hard-scattering processes is written as the convolution of the parton distributions  $f_{i/h}$ , the  $C$  functions (representing the finite pieces of the virtual corrections), and two Sudakov form factors,  $\mathcal{S}^P$  and  $\mathcal{S}^{NP}$ .  $\mathcal{S}^P$  can be regarded as being perturbative in character and  $\mathcal{S}^{NP}$  as non-perturbative. The perturbative Sudakov form factor represents a formal resummation of soft-gluon emissions. The non-perturbative Sudakov form factor is determined from a fit to the data, is expected to be universal (for a given parton flavor and hadron type), and is usually parameterized as a Gaussian distribution. The dividing line between the perturbative and non-perturbative contributions is somewhat arbitrary (similar to the better known cases of parton distributions and fragmentation functions), and it is quantified by a theoretical scale in the resummation formalism. The  $p_T$  distribution (e.g., of the Drell-Yan pair) can be written symbolically as

$$\frac{d\sigma}{dp_T} = \sigma_0 e^{-(\mathcal{S}^{NP} + \mathcal{S}^P)} \otimes \left[ \left( C_{a_1 i} \otimes f_{i/h_1} \right) \left( C_{a_2 j} \otimes f_{j/h_2} \right) \right] + Y. \quad (1)$$

The  $Y$  function is added to ensure a smooth matching between the low and the high- $p_T$  regions, where the resummed and the fixed-order descriptions work better, respectively.

At collider energies, most of the  $k_T$  can be attributed to perturbative soft-gluon emission. However, for fixed-target kinematics, almost all of the  $k_T$  is due to the non-perturbative

mechanisms. A proper treatment requires both the appropriate data to determine the non-perturbative input, and an implementation of the soft-gluon resummation formalism for the particular process.

The resummation calculation for multiple soft-gluon emission in direct-photon production is quite challenging. The production rate and kinematic distributions of photon pairs produced in hadron interactions have already been calculated [16], and a similar calculation of the transverse momentum distribution of a photon-jet system is also plausible, but more involved, since the final-state parton takes part in soft-gluon emission and in color exchange with the initial-state partons. A recent work on this subject [20] addressed only the effects of multiple soft-gluon radiation in the initial state. Incorporating jet definition in the formalism is also not a fully resolved issue. Finally, the calculation of individual transverse momenta of the photon and the jet is further complicated by the fact that several overlapping power-suppressed corrections can contribute. In the absence of the full resummed calculation, approximations are made in order to compare theory with data.

In lieu of a rigorous calculation of the resummed  $p_T$  distribution, effects of soft-gluon radiation can be approximated by a convolution of the leading-order cross section with a  $k_T$ -smearing function [21]. In the formalism described above, this is equivalent to absorbing all of the perturbative gluon emissions into the non-perturbative Sudakov form factor. Since no explicit resummation of soft-gluon emissions is performed, the average value of  $k_T$  used in the smearing should be representative of the value observed (or expected) in the kinematic regime of the experiment.

The expression for the leading-order (LO) cross section for direct-photon production at large  $p_T$  has the form:

$$E_\gamma \frac{d^3\sigma}{dp^3}(h_1 h_2 \rightarrow \gamma X) = \sum_{a_1 a_2 a_3} \int dx_1 dx_2 f_{a_1/h_1}(x_1, Q^2) f_{a_2/h_2}(x_2, Q^2) \frac{\hat{s}}{\pi} \frac{d\sigma}{d\hat{t}}(a_1 a_2 \rightarrow \gamma a_3) \delta(\hat{s} + \hat{t} + \hat{u}), \quad (2)$$

where  $d\sigma/d\hat{t}$  is the hard-scattering matrix element, and  $f_{a_1/h_1}$  and  $f_{a_2/h_2}$  are the parton distribution functions (pdf) for the colliding partons  $a_1$  and  $a_2$  in hadrons  $h_1$  and  $h_2$ , re-

spectively. To introduce  $k_T$  degrees of freedom, one extends each integral over the parton distribution functions to the  $k_T$ -space,

$$dx_1 f_{a_1/h_1}(x_1, Q^2) \rightarrow dx_1 d^2k_{T_1} g(\vec{k}_{T_1}) f_{a_1/h_1}(x_1, Q^2), \quad (3)$$

(a corresponding substitution is done for parton  $a_2$  in hadron  $h_2$ ).

The distribution  $g(\vec{k}_T)$  is usually taken to be a Gaussian,

$$g(\vec{k}_T) = \frac{e^{-k_T^2/\langle k_T^2 \rangle}}{\pi \langle k_T^2 \rangle}, \quad (4)$$

where  $\langle k_T^2 \rangle$  is the square of the 2-dimensional (2D) RMS width of the  $k_T$  distribution for one parton ( $\sigma_{1parton,2D}^2$ ), and is related to the square of the 2D average of the absolute value of  $\vec{k}_T$  of one parton through  $\langle k_T^2 \rangle = 4\langle k_T \rangle^2/\pi$ . We emphasize that  $\langle k_T \rangle$  represents the average effective 2D transverse momentum per parton. (The average transverse momentum of the parton pair is, of course, a factor of  $\sqrt{2}$  larger than the average transverse momentum per parton.)

The 4-vectors of the colliding partons are expressed in terms of the momentum fraction  $x$  of the partons. Ignoring parton and hadron masses,

$$x_1 = (E_1 + p_{l_1})/\sqrt{s}, \quad (5)$$

where the parton four-vector is

$$p_1 = (E_1, \vec{k}_{T_1}, p_{l_1}), \quad (6)$$

with

$$E_1 = \frac{1}{2} \left[ x_1 \sqrt{s} + \frac{k_{T_1}^2}{x_1 \sqrt{s}} \right], \quad (7)$$

and

$$p_{l_1} = \frac{1}{2} \left[ x_1 \sqrt{s} - \frac{k_{T_1}^2}{x_1 \sqrt{s}} \right]. \quad (8)$$

(Similar expressions are used for parton  $a_2$ .)

It is straightforward to evaluate the invariant cross sections, including  $k_T$  effects, according to the above prescription. In general, because the unmodified PQCD cross sections fall rapidly with increasing  $p_T$ , the net effect of the  $k_T$  smearing is to increase the yield. We denote the enhancement factor as  $K(p_T)$ . Since the invariant cross section for direct-photon production is now a six-dimensional integral, it is convenient to employ Monte Carlo techniques in the evaluation of  $K(p_T)$ . An exact treatment of the kinematics can be implemented in a Monte Carlo framework, but it is more difficult in an analytic approach.

A Monte Carlo program that includes such a treatment of  $k_T$  smearing, and the leading-order cross section for high- $p_T$  particle production, has long been available [21]. The program provides calculations of many experimental observables, in addition to inclusive cross sections. The program can be used for direct photons, jets, and for single high- $p_T$  particles resulting from jet fragmentation (such as inclusive  $\pi^0$  production). Unfortunately, no such program is available for NLO calculations, but one can approximate the effect of  $k_T$  smearing by multiplying the NLO cross sections by the LO  $k_T$ -enhancement factor. Admittedly, this procedure involves a risk of double-counting since some of the  $k_T$ -enhancement may already be contained in the NLO calculation. However, such double-counting effects are expected to be small, and consequently this uncertainty on  $K(p_T)$  should also be small. (For example, the NLO estimate for  $\langle p_T \rangle_{pair}$  of the diphoton pairs produced in  $pp \rightarrow \gamma\gamma$  at  $\sqrt{s} = 31.5$  GeV is on the order of a few hundred MeV/ $c$ , while the resummed prediction is well over 1 GeV/ $c$  [14].)

It is clear that this type of treatment of  $k_T$  effects is model dependent. In particular, different functional forms can lead to quantitatively different answers. For example, adding substantial non-Gaussian tails in  $k_T$  smearing can affect the output distributions. One of the strengths of the approach we follow in this paper is that the  $k_T$  distribution used in the smearing is based on experimental information, and the Gaussian character of the  $k_T$  effects is consistent with the data observed by E706 [9]. Moreover, any non-Gaussian tails may result primarily from single hard-gluon emission, and such contributions should therefore already be contained in the NLO cross sections used in this analysis.

A complete treatment of soft-gluon radiation in high- $p_T$  production, including the appropriate non-perturbative input, should eventually predict the effective  $k_T$  values expected for each process and  $\sqrt{s}$ . We will employ  $\langle k_T \rangle$  values representative of the kinematic distributions in the data, and based on comparisons with the same model as used to modify the NLO inclusive cross sections.

The effects of soft-gluon radiation are also included in QCD Monte Carlo programs such as PYTHIA [22], ISAJET [23], and HERWIG [24]. However, in these programs the emission is normally cut off at a relatively high parton virtuality, with the remaining  $k_T$  effect supplied by a Gaussian smearing similar to that discussed above. For fixed-target energies, essentially all of the  $k_T$  effects are provided by this phenomenological Gaussian term. The above programs differ in the details of the way parton energy and momentum are rescaled after  $k_T$  is inserted, which can also produce quantitative differences in results.

## APPLICATIONS OF THE $k_T$ MODEL TO DATA

The experimental consequences of  $k_T$  smearing are expected to depend on the collision energy. At the Tevatron collider, the smallest photon  $p_T$  values probed by the CDF and DØ experiments are rather large (10–15 GeV/ $c$ ), and the  $k_T$ -enhancement factors modify only the very lowest end of the  $p_T$  spectrum, where  $p_T$  is not significantly larger than  $k_T$ . In the energy range of the E706 measurements, large  $k_T$ -effects can modify both the normalizations and the shapes of the cross sections as functions of  $p_T$ . Consequently, E706 data provide a particularly sensitive test of the  $k_T$  model. At lower fixed-target energies, the  $k_T$  enhancements are expected to have less  $p_T$  dependence over the range of available measurements, and can therefore be masked more easily by uncertainties in experimental normalizations and/or choices of theoretical scales. Nonetheless, the UA6 and WA70 data generally support the expectations from  $k_T$  smearing.



## Comparisons to Tevatron Collider Data

At the Tevatron collider, the above model of soft-gluon radiation leads to a relatively simple modification of the NLO cross section. In Fig. 2 we compare the CDF and DØ isolated direct-photon cross sections [25] to theoretical NLO calculations with and without  $k_T$  enhancement. In the lower part of the plot we display the quantity (Data–Theory)/Theory; for the collider regime we did not multiply the NLO theory by the  $k_T$ -enhancement factor, but instead displayed the full deviation of the NLO calculation from the data. The expected effect from  $k_T$  enhancement is also shown for  $\langle k_T \rangle = 3.5 \text{ GeV}/c$ . This is the approximate value of  $\langle k_T \rangle$  per parton measured in diphoton production at the Tevatron [25], and one expects a similar  $\langle k_T \rangle$  per parton for single-photon production. (In the diphoton process, the 4-vectors of the photons can be measured precisely, providing a direct determination of the transverse momentum of the diphoton system, and thereby  $\langle k_T \rangle$ .)

As seen in Fig. 2, the  $k_T$  effect diminishes rapidly with  $p_T$  and is essentially negligible above  $\approx 30 \text{ GeV}/c$ . The trend of deviations of NLO calculations from the measured inclusive cross sections is described reasonably well by the expected  $k_T$  effect. Some of the observed excess can be attributed to the fragmentation contribution to isolated direct-photon production [26], but this alone cannot account for the entire deviation of the theory from data.

The larger statistics in the Tevatron collider Run IB samples (currently under analysis) will allow for a more detailed examination of the low- $p_T$  behavior of the photon cross section. (The CDF data included in the plot are from Run IA only.) A similar enhancement is expected for jet production at low  $p_T$ , but larger experimental uncertainties, and the relatively large additional non-perturbative effects expected in this region [27], preclude a useful comparison.

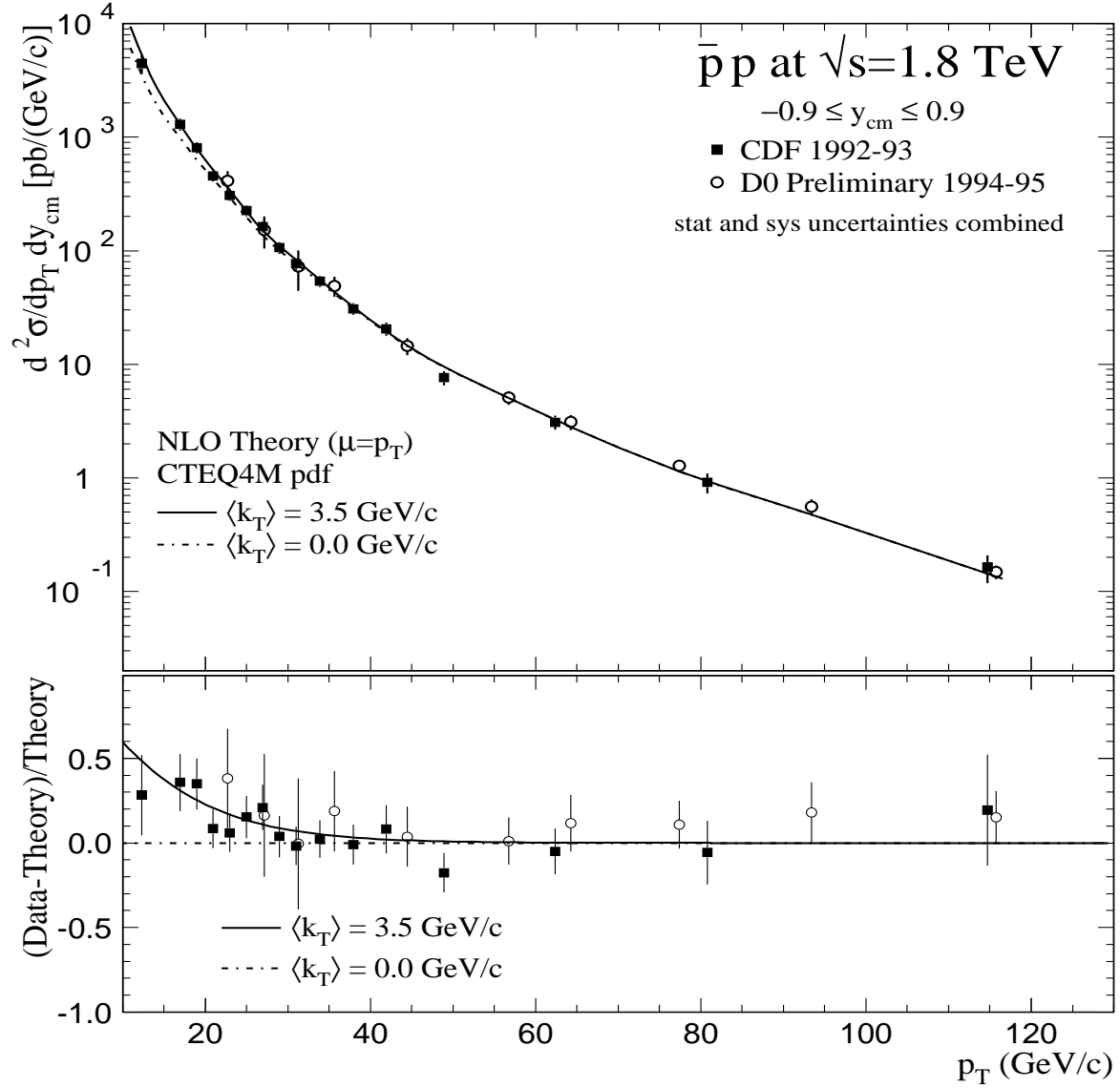


FIG. 2. Top: The CDF and DØ isolated direct-photon cross sections, compared to NLO theory without  $k_T$  (dashed) and with  $k_T$  enhancement for  $\langle k_T \rangle = 3.5$  GeV/ $c$  (solid), as a function of  $p_T$ . Bottom: The quantity (Data-Theory)/Theory (for theory without  $k_T$  adjustment), overlaid with the expected effect from  $k_T$  enhancement for  $\langle k_T \rangle = 3.5$  GeV/ $c$ . The error bars have experimental statistical and systematic uncertainties added in quadrature.

## Comparisons to E706 Data

The conventional NLO calculations yield cross sections that are significantly below the E706 direct-photon and  $\pi^0$  measurements [9] (see Figs. 3, 4, and 5). No choices of current parton distributions, or conventional PQCD scales provide an adequate description of the data (for the comparisons presented here all QCD scales have been set to  $p_T/2$ ). The previously described  $k_T$ -enhancement algorithm was used to incorporate the effects of soft-gluon radiation in the calculated yields. That is, the theory results plotted in the figures represent the NLO calculations multiplied by  $k_T$ -enhancement factors  $K(p_T)$  [28].

Because parton distributions for nucleons are known better than those for pions, we first present comparisons of the various model calculations with proton-beam data. As seen at the bottoms of Figs. 3 and 4, the NLO theory, when supplemented with appropriate  $k_T$  enhancements, is successful in describing both the shape and normalization of the E706 direct-photon cross sections at both  $\sqrt{s} = 31.6$  GeV and 38.8 GeV. As expected, the  $k_T$ -enhancement factors affect the normalization of the cross sections, as well as the shapes of the  $p_T$  distributions. The values of  $\langle k_T \rangle = 1.2$  GeV/ $c$  at  $\sqrt{s} = 31.6$  GeV, and 1.3 GeV/ $c$  at  $\sqrt{s} = 38.8$  GeV, provide good representations of the incident-proton data. Both  $k_T$  values are consistent with those emerging from a comparison of the same PQCD Monte Carlo with E706 data on the production of high-mass  $\pi^0\pi^0$ ,  $\gamma\pi^0$  and  $\gamma\gamma$  pairs [9].

In Fig. 5 we present comparisons between calculations and E706 data for  $\pi^-$ Be interactions at  $\sqrt{s} = 31.1$  GeV. Here again, the uncorrected ( $\langle k_T \rangle = 0$ ) NLO theory is not consistent with the data. Once the  $k_T$ -enhancement factors are applied, good agreement is observed between data and calculations for  $\langle k_T \rangle \approx 1.4$  GeV/ $c$ . (Note that DY data lead one to expect a higher value of  $\langle k_T \rangle$  for a  $\pi^-$  beam than for a proton beam of the same energy.)

For comparison, results of calculations using  $\langle k_T \rangle$  values  $\pm 0.2$  GeV/ $c$  of the central values are also shown in the figures. These can be taken as an indication of uncertainties on  $\langle k_T \rangle$  (see next section). The corresponding enhancement factors  $K(p_T)$  at  $\sqrt{s} = 31.6$  GeV are displayed in Fig. 6.

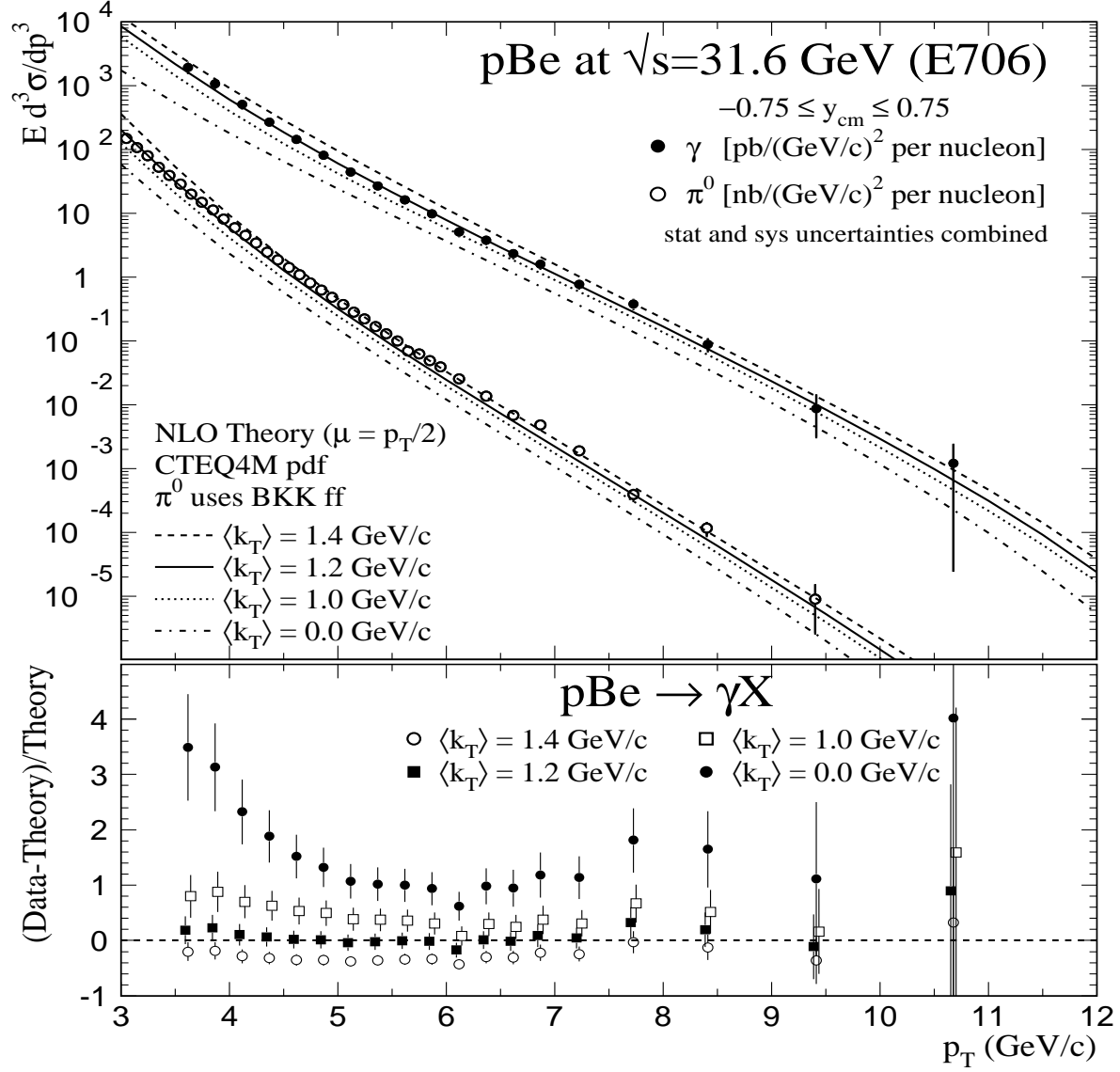


FIG. 3. Top: The photon and  $\pi^0$  cross sections from E706 at  $\sqrt{s} = 31.6$  GeV compared to  $k_T$ -enhanced NLO calculations. Bottom: The quantity (Data-Theory)/Theory for direct-photon production, using  $k_T$ -enhanced NLO calculations for several values of  $\langle k_T \rangle$ . The error bars have experimental statistical and systematic uncertainties added in quadrature. The points corresponding to calculations with different  $\langle k_T \rangle$  are slightly staggered in  $p_T$ , to reduce the overlap of experimental error bars.

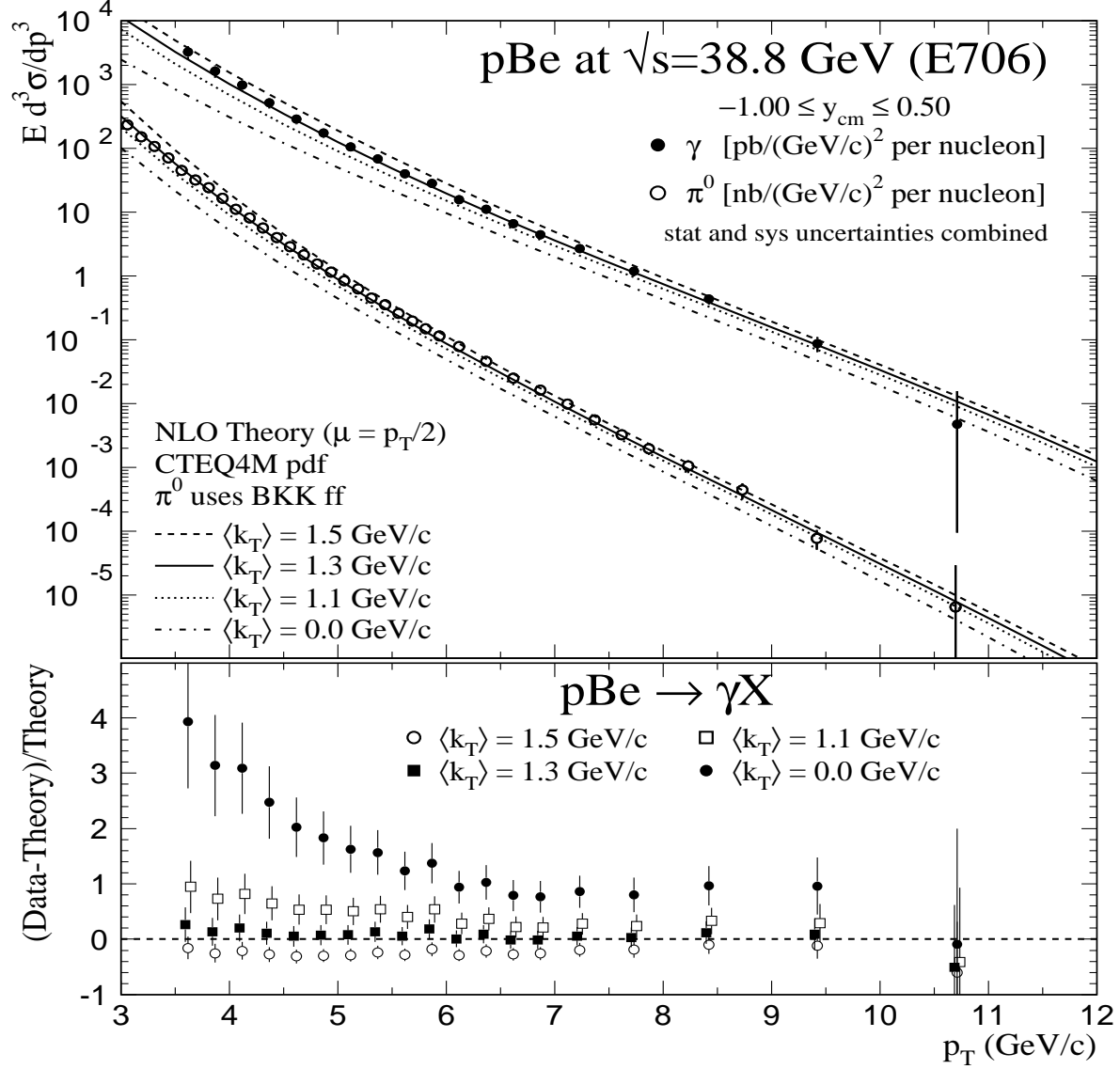


FIG. 4. Top: The photon and  $\pi^0$  cross sections from E706 at  $\sqrt{s} = 38.8$  GeV compared to  $k_T$ -enhanced NLO calculations. Bottom: The quantity (Data-Theory)/Theory for direct-photon production, using  $k_T$ -enhanced NLO calculations for several values of  $\langle k_T \rangle$ . The error bars have experimental statistical and systematic uncertainties added in quadrature.

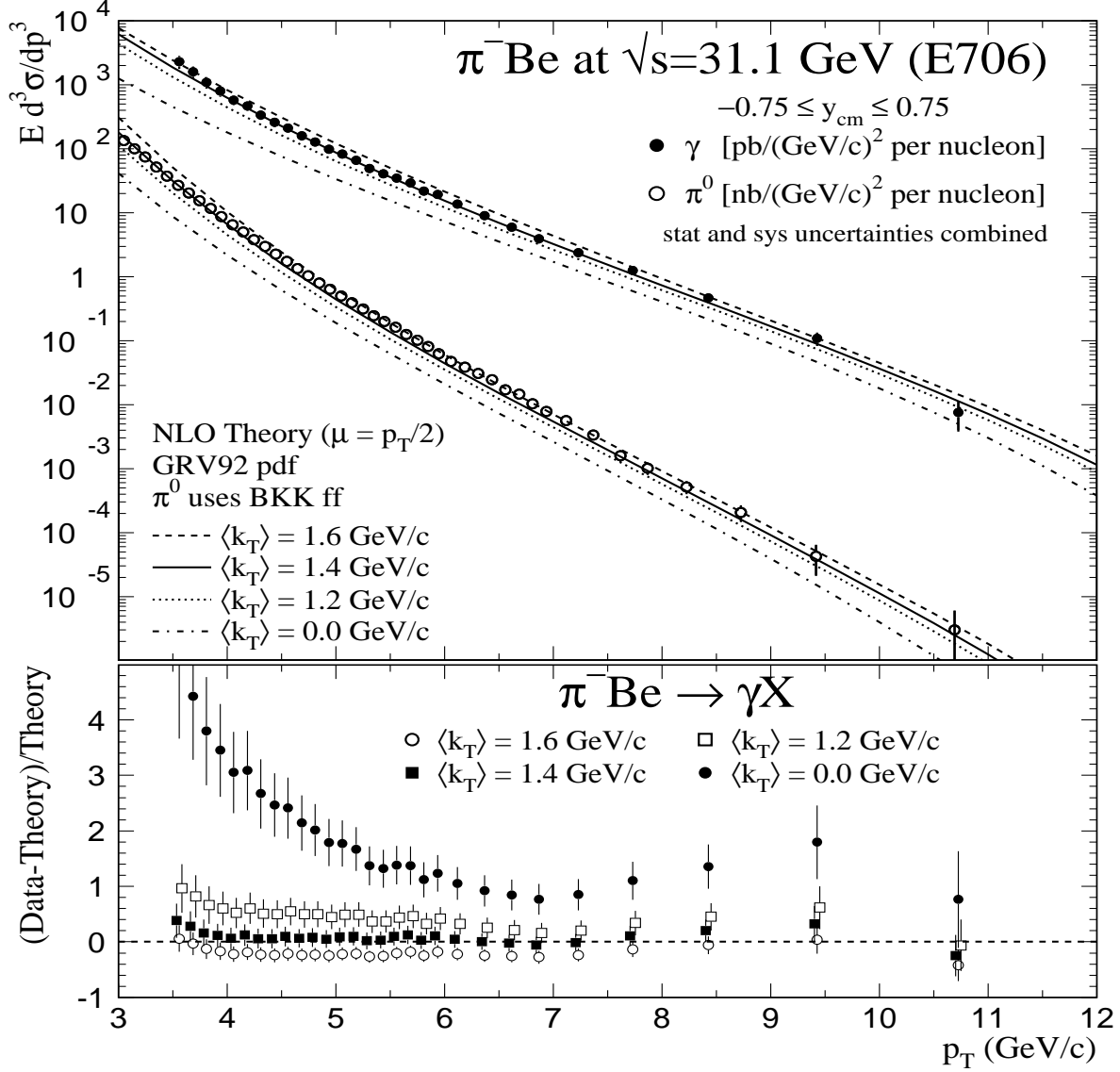


FIG. 5. Top: The photon and  $\pi^0$  cross sections from E706 at  $\sqrt{s} = 31.1 \text{ GeV}$  for incident  $\pi^-$  beam, compared to  $k_T$ -enhanced NLO calculations. Bottom: The quantity (Data-Theory)/Theory for direct-photon production, using  $k_T$ -enhanced NLO calculations for several values of  $\langle k_T \rangle$ . The error bars have experimental statistical and systematic uncertainties added in quadrature.

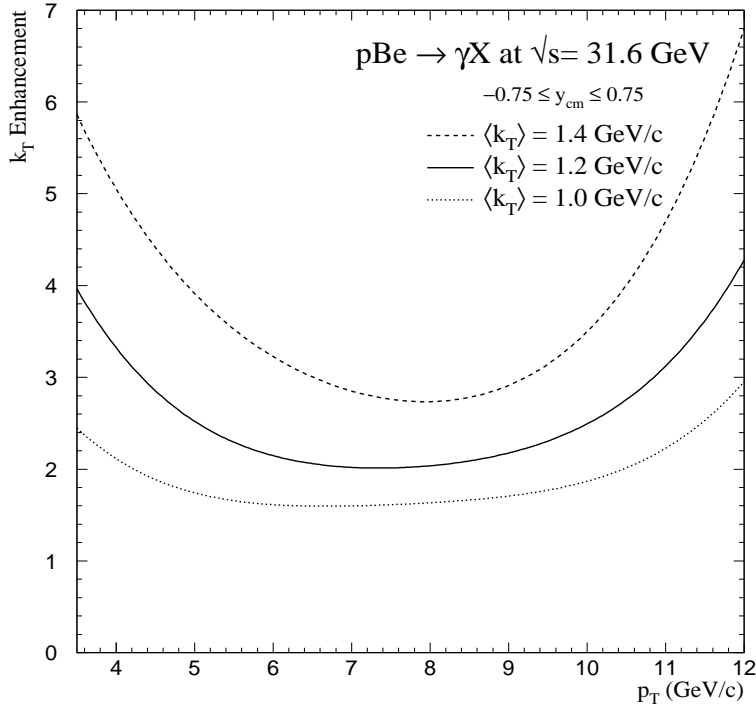


FIG. 6. The variation of  $k_T$  enhancements,  $K(p_T)$ , relevant to the E706 direct-photon data for protons at  $\sqrt{s} = 31.6$  GeV, for different values of  $\langle k_T \rangle$ .

It is interesting to note that, in this energy range, the  $k_T$  enhancement does not decrease with increasing  $p_T$  (as for the case of the collider), and, in fact, increases at the highest values of  $p_T$ . This is a consequence of the wide  $x$ -range spanned by E706, and can be understood through the following argument. At low  $p_T$ , a  $\langle k_T \rangle$  of 1.2 GeV/c is non-negligible in comparison to the  $p_T$  in the hard-scattering, and the addition of  $k_T$  smearing therefore increases the size of the cross section (and steepens the slope). At high  $p_T$  (corresponding to large  $x$ ), the unmodified NLO cross section becomes increasingly steep (due to the rapid fall in parton densities), and hence the effect of  $k_T$  smearing again becomes larger.

NLO calculations for  $\pi^0$  production have a greater theoretical uncertainty than those for direct-photon cross sections since they involve parton fragmentation. However, the  $k_T$  effects in  $\pi^0$  production can be expected to be generally similar to those observed in direct-photon production, and the  $\pi^0$  data can be used to extend tests of the consequences of  $k_T$  smearing.

Figures 3, 4, and 5 also show comparisons between NLO calculations [29] and  $\pi^0$  production from E706, using BKK fragmentation functions (ff) [30]. The previously described Monte Carlo program was employed to generate  $k_T$ -enhancement factors for  $\pi^0$  cross sections, and  $\langle k_T \rangle$  per parton values similar to those that resulted in good agreement with direct-photon data also provide a reasonable description of  $\pi^0$  production. For  $\pi^0$  production, an additional smearing of the transverse momentum, expected from jet fragmentation, has been taken into account.

### Comparisons to WA70 and UA6 Data

We have examined the expectations for the size of soft-gluon effects for fixed-target experiments WA70 and UA6. Both experiments have measured direct-photon production with good statistics, and their data have been included in recent global fits to parton distributions. WA70 measured direct-photon and  $\pi^0$  production in  $pp$  and  $\pi^-p$  collisions at  $\sqrt{s} = 23.0$  GeV [31], and UA6 has recently released [10] their final results (with substantially reduced uncertainties) for direct-photon production in  $pp$  and  $\bar{p}p$  collisions at  $\sqrt{s} = 24.3$  GeV. These center of mass energies are somewhat smaller than those of E706, and the  $\langle k_T \rangle$  values are therefore expected to be smaller (perhaps of the order of 0.7–0.9 GeV/ $c$ , based on Fig. 1). WA70 has compared kinematic distributions observed in diphoton events (for  $\pi^-p$  interactions) to NLO predictions, and has found that smearing the NLO theory with an additional  $\langle k_T \rangle$  of  $0.9 \pm 0.2$  GeV/ $c$  provides agreement with their data [32]. We therefore use this  $\langle k_T \rangle$  as the central value for the  $k_T$ -enhancement factors for both experiments, and vary the  $\langle k_T \rangle$  by  $\pm 0.2$  GeV/ $c$ , as with E706. The corresponding  $k_T$  enhancement expected over the range of measurements is shown in Fig. 7. Over this narrower  $p_T$  range, the effect of  $k_T$  is essentially to produce a shift in normalization.

Comparisons of the WA70 direct-photon and  $\pi^0$  cross sections with the  $k_T$ -enhanced NLO calculations are shown in Figs. 8 and 9. Renormalization and factorization scales of  $p_T/2$  are used in the NLO calculations, as in the E706 comparisons. The  $\pi^0$  cross sections



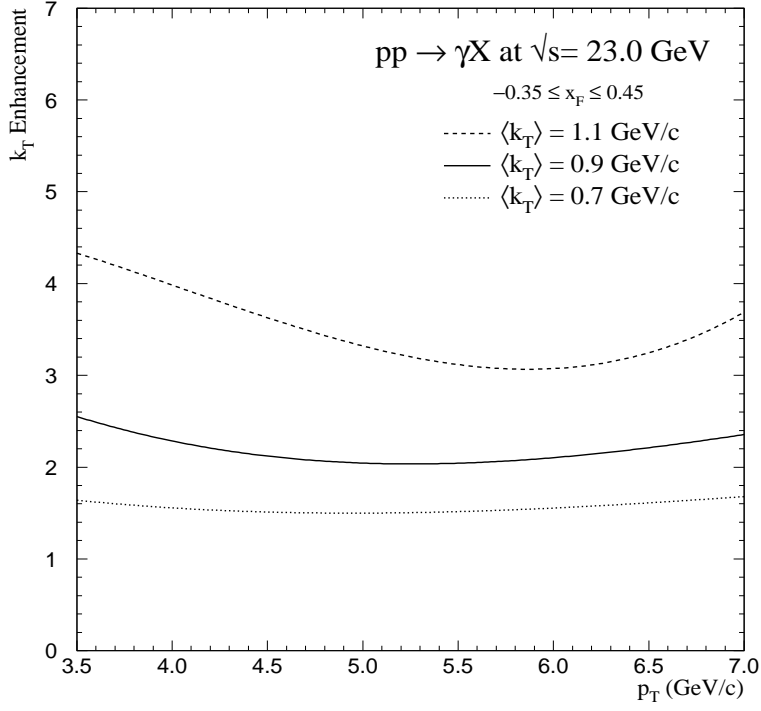


FIG. 7. The  $k_T$ -enhancement factors for direct-photon production expected for WA70  $pp$  data.

both for incident proton and  $\pi^-$  beams, and the photon data from incident  $\pi^-$  beam, all lie above the NLO calculations for  $\langle k_T \rangle = 0$ , and are in better agreement with the  $k_T$ -enhanced calculations; only the photon cross section for incident protons seems not to require a  $k_T$  correction.

The latest photon cross sections from UA6 for  $pp$  and  $\bar{p}p$  scattering are shown in Figs. 10 and 11. The photon cross section for  $pp$  interactions lies clearly above the NLO calculation for  $\langle k_T \rangle = 0$ , but is consistent with  $k_T$ -adjusted calculations for  $\langle k_T \rangle$  in the range of 0.7–0.9 GeV/ $c$ . The result for  $\bar{p}p$  interactions is also above the unmodified NLO calculation, but requires a smaller value of  $\langle k_T \rangle$ . We note that the dominant production mechanisms for the two processes are different: quark-gluon Compton scattering dominates for  $pp$ , and  $\bar{q}q$  annihilation for  $\bar{p}p$  at the UA6 energy. As in the case of E706 and WA70 measurements, the UA6  $\pi^0$  cross sections are also higher than the NLO calculation without  $k_T$ , and can be much better described by introducing  $k_T$  enhancement.

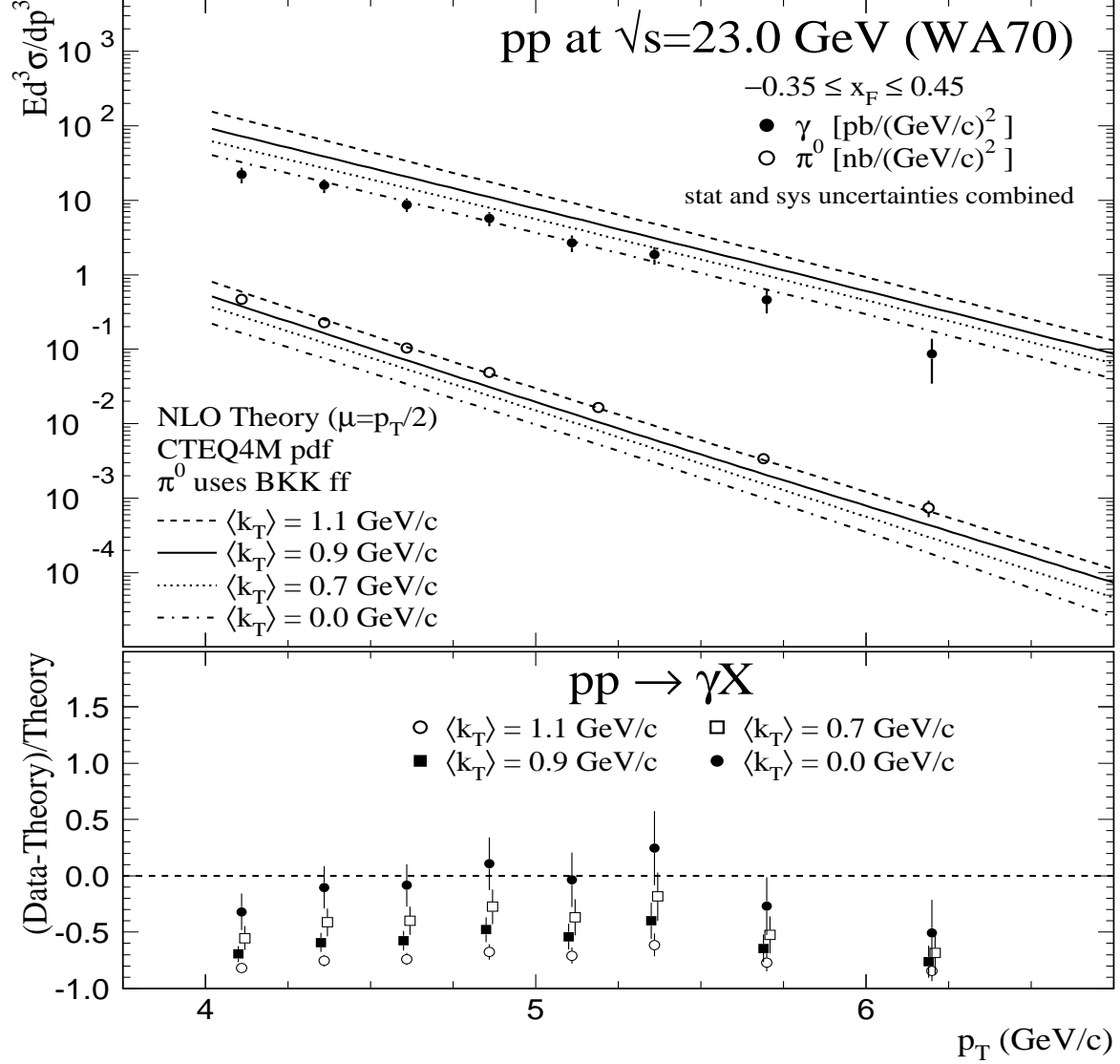


FIG. 8. Top: The photon and  $\pi^0$  cross sections from WA70 at  $\sqrt{s} = 23.0$  GeV for incident protons compared to  $k_T$ -enhanced NLO calculations. Bottom: The quantity  $(\text{Data} - \text{Theory}) / \text{Theory}$  for direct-photon production, using  $k_T$ -enhanced NLO calculations for several values of  $\langle k_T \rangle$ . The error bars have experimental statistical and systematic uncertainties added in quadrature.

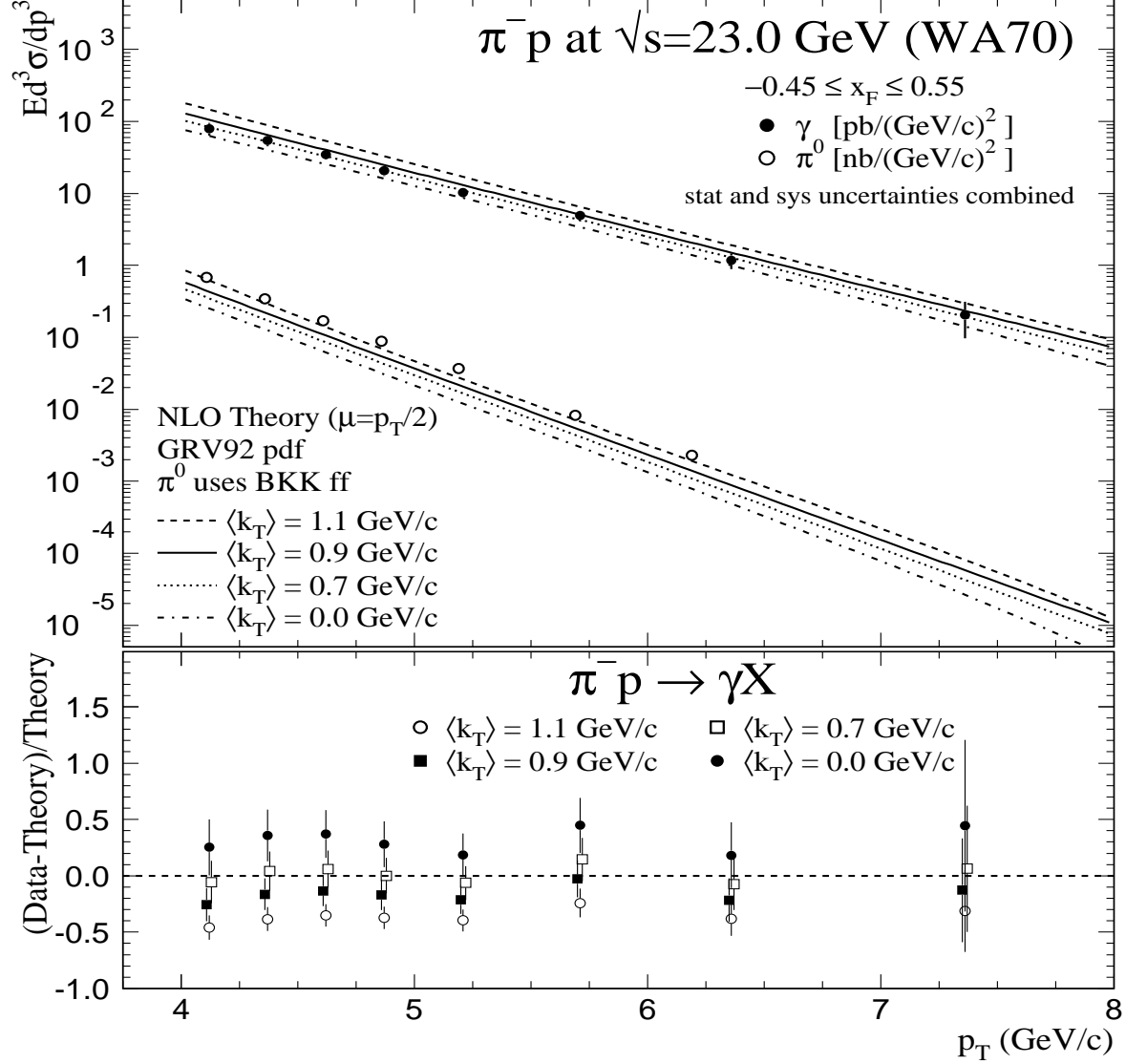


FIG. 9. Top: The photon and  $\pi^0$  cross sections from WA70 at  $\sqrt{s} = 23.0$  GeV for incident  $\pi^-$  beam, compared to  $k_T$ -enhanced NLO calculations. Bottom: The quantity (Data-Theory)/Theory for direct-photon production, using  $k_T$ -enhanced NLO calculations for several values of  $\langle k_T \rangle$ . The error bars have experimental statistical and systematic uncertainties added in quadrature.

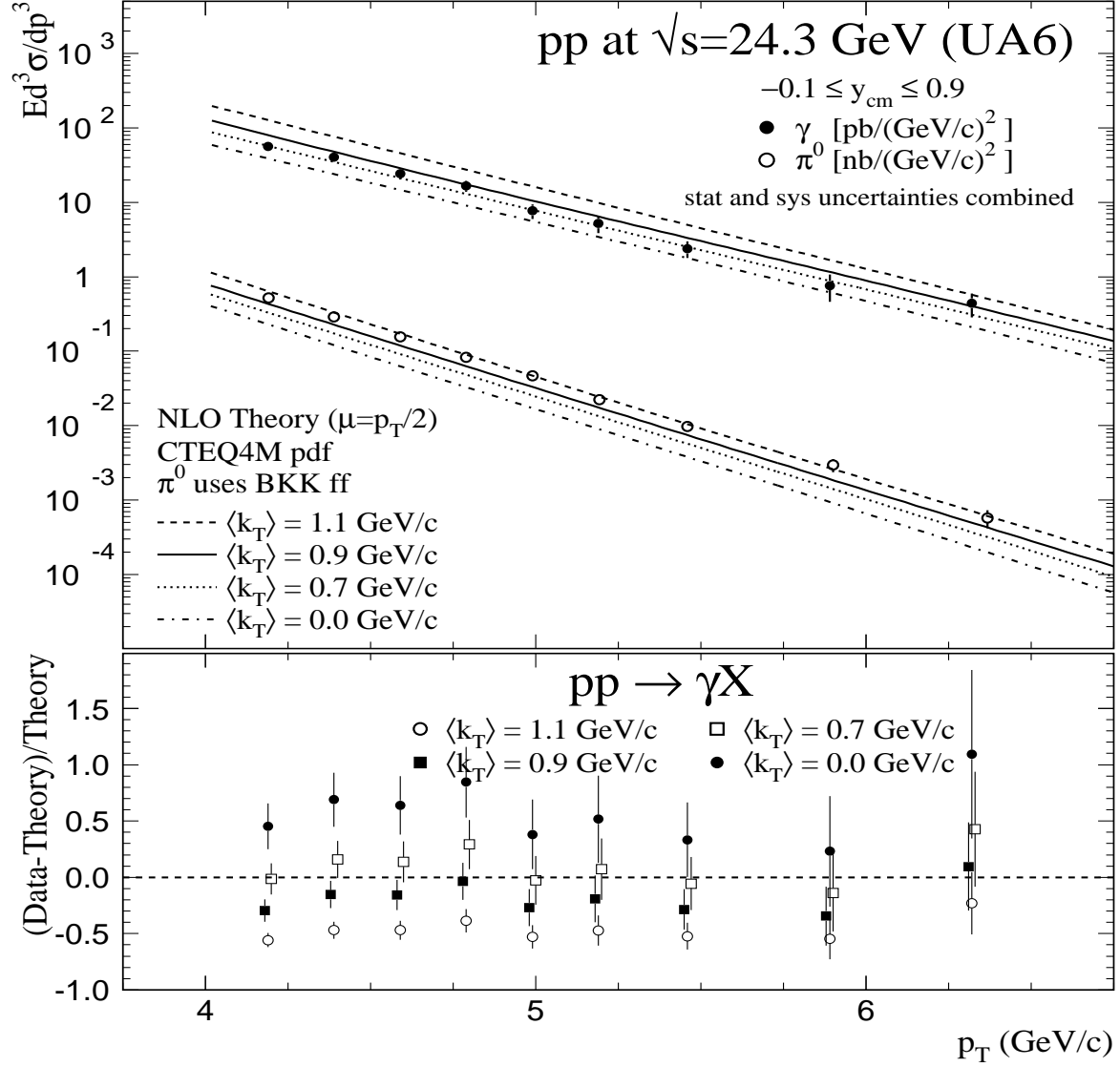


FIG. 10. Top: The photon and  $\pi^0$  cross sections from UA6 at  $\sqrt{s} = 24.3$  GeV for an incident proton beam compared to  $k_T$ -enhanced NLO calculations. Bottom: The quantity  $(\text{Data} - \text{Theory}) / \text{Theory}$  for direct-photon production, using  $k_T$ -enhanced NLO calculations for several values of  $\langle k_T \rangle$ . The error bars have experimental statistical and systematic uncertainties added in quadrature.

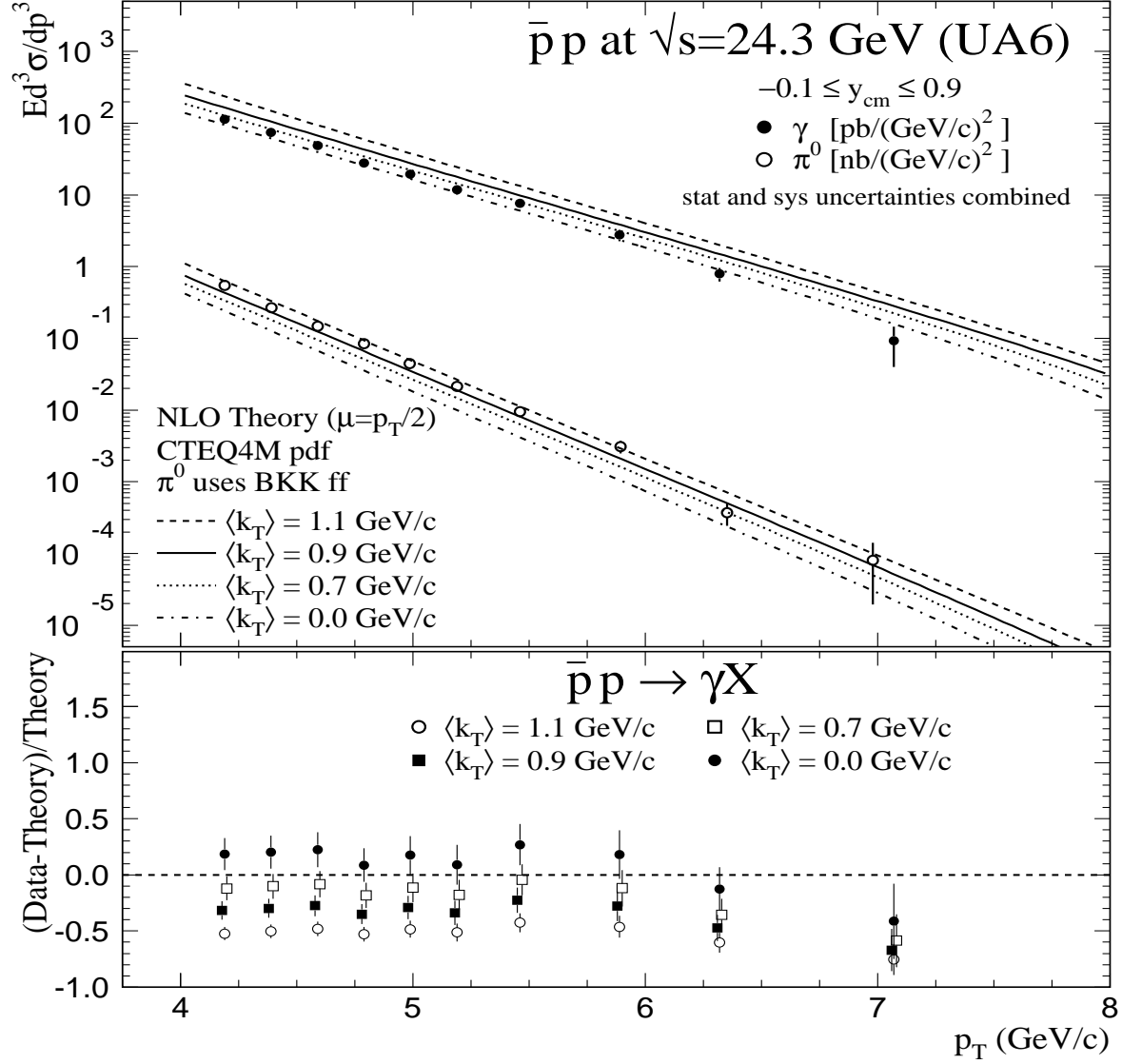


FIG. 11. Top: The photon and  $\pi^0$  cross sections from UA6 at  $\sqrt{s} = 24.3$  GeV for an incident antiproton beam compared to  $k_T$ -enhanced NLO calculations. Bottom: The quantity  $(\text{Data} - \text{Theory}) / \text{Theory}$  for direct-photon production, using  $k_T$ -enhanced NLO calculations for several values of  $\langle k_T \rangle$ . The error bars have experimental statistical and systematic uncertainties added in quadrature.

## DISCUSSION OF $k_T$ -SMEARING PROCEDURES

In this section, we consider uncertainties in the Monte Carlo method employed in our previous discussion, and comment on an analytic approach for calculating such  $k_T$  enhancements.

### Uncertainties in the Monte Carlo Model and Related Issues

Our approach contains several phenomenological parameters that affect the range of its results, the most important of which is the amount of Gaussian smearing represented by  $\langle k_T \rangle$ . Thus far, both the value of  $\langle k_T \rangle$  (with its dependence on  $\sqrt{s}$ ) and its possible range of uncertainty can only be determined empirically. A range of variation of  $\pm 0.2$  GeV/ $c$  for  $\langle k_T \rangle \sim 1\text{--}2$  GeV/ $c$  appears reasonable on the basis of several considerations. These include: (i) the range of  $k_T$  values inferred from the E706 high-mass pair distributions for several kinematic variables; (ii) observed differences between photon and  $\pi^0$  results; (iii) comparisons of  $\langle k_T \rangle$  values required in inclusive cross sections to those representing the properties of massive pairs at E706 and WA70/UA6 energies, and (iv) differences between dimuon, diphoton, and dijet values of  $\langle p_T \rangle_{pair}$ . (The dependence of the  $k_T$ -enhancement factor on the variation in  $\langle k_T \rangle$  was illustrated in Figs. 6 and 7.)

For the fixed-target experiments discussed in the previous section, we already presented calculations using  $\langle k_T \rangle$  values of 0.2 GeV/ $c$  above and below the selected central values. The observed variation in predictions reflects an uncertainty in the  $k_T$ -enhanced theoretical results. The dependence of  $K(p_T)$  on  $\langle k_T \rangle$  is especially strong at the extremes (low and high) in  $p_T$ . These calculations used renormalization and factorization scales of  $p_T/2$ . Changing the scale to  $p_T$  reduces predicted cross sections at fixed-target energies by about 30–40%, a factor comparable to the estimated spread in the  $k_T$  factors over much of the  $p_T$  range; the full uncertainty in the calculations must include contributions from uncertainties in both  $\langle k_T \rangle$  and QCD scales.

Another parameter in the model, a propagator mass  $m$ , is introduced to regularize the divergences of the leading-order QCD matrix elements due to the propagator factors  $1/\hat{s}$ ,  $1/\hat{t}$ , and  $1/\hat{u}$  in the configuration where one or more of these invariants approaches zero. To avoid the large weights associated with these configurations, the propagators are replaced by  $1/(\hat{s} + m^2)$ ,  $1/(\hat{t} - m^2)$ , and  $1/(\hat{u} - m^2)$ , respectively, where  $m$  has a typical value of order 1 GeV. The physical effect of the propagator mass is to cut off the region where almost all of the transverse momentum of the produced photon is due to the Gaussian smearing, and very little to the hard scattering. While the  $k_T$ -enhancement factor is relatively insensitive to the value of  $m$  for the measured range at collider energies, it is somewhat sensitive for data at fixed-target energies.

To illustrate the sensitivity of the  $k_T$ -enhancement factor  $K(p_T)$  to the choice of the propagator mass, we display in Fig. 12 the results for  $m = 1.0$  GeV (default value), 1.3 GeV, and 0, for  $p\text{Be} \rightarrow \gamma X$  at  $\sqrt{s} = 31.6$  GeV. Above  $p_T$  values of 5.5–6.0 GeV/ $c$ , the  $k_T$  enhancement has little sensitivity to  $m$ . At lower  $p_T$ , the dependence on the propagator mass should be considered as a measure of an uncertainty of the model in this region of phase space. Clearly, larger enhancements are obtained at low  $p_T$  when there is no propagator mass ( $m = 0$ ).

The value of  $\langle k_T \rangle$ , appropriate in the calculation, depends on the kinematic situation. The increase of the value of  $\langle k_T \rangle$  with  $s$  is understood, in general terms, as the result of an increase in the available phase space for multiple-soft-gluon emission. This growth is predicted by a CSS-type of resummation for Drell-Yan processes [33] and, as illustrated in Fig. 1, has been observed in Drell-Yan and diphoton data. For simplicity, the model calculation assumes a constant value of  $\langle k_T \rangle$  for a given  $\sqrt{s}$ . In reality, various physical effects can modify this simple choice and cause a modification in the shape of the enhancement factor  $K(p_T)$ . Below, we discuss a few of these effects.

First, one might expect a dependence of  $\langle k_T \rangle$  on  $\hat{s}$ , the hardness of the partonic interaction, similar to that on  $s$ . A study of diphoton production at  $\sqrt{s} = 31.5$  GeV, using the RESBOS program [14], indicates that the  $\langle k_T \rangle$  increases from about 1.2 GeV/ $c$  for photons

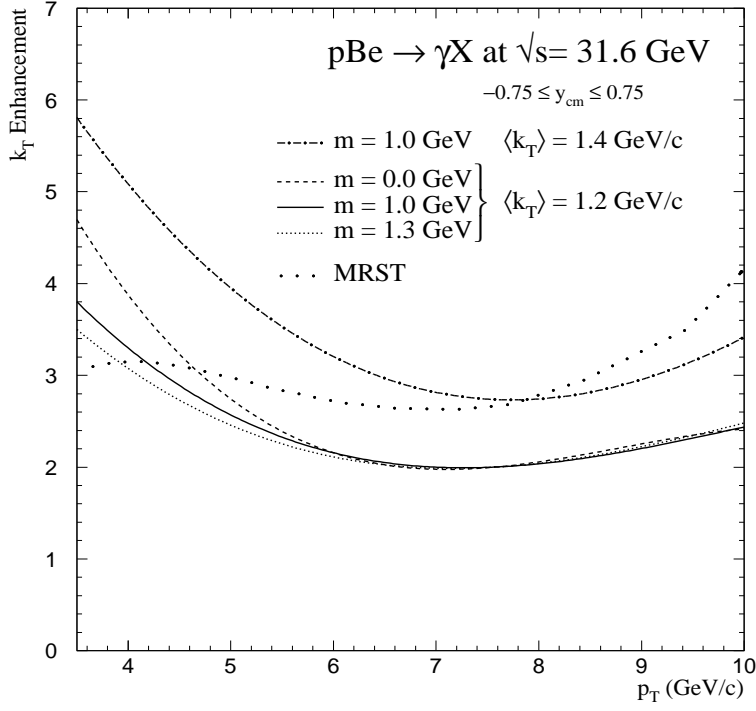


FIG. 12. The effect of different propagator masses  $m$  for predictions of  $k_T$  enhancements  $K(p_T)$  for E706 direct-photon data at  $\sqrt{s} = 31.6$  GeV. The  $k_T$  enhancement used by the MRST group [36] is also shown in the figure.

with  $p_T$  of 5 GeV/ $c$  to approximately 1.4 GeV/ $c$  for photons with  $p_T$  of 10 GeV/ $c$ . If direct-photon production were to have a similar behavior, the anticipated  $k_T$  enhancement at a  $p_T$  of 10 GeV/ $c$  would be about 40% higher than for a constant  $\langle k_T \rangle$  value of 1.2 GeV/ $c$  (see the dependence of the enhancement factor on  $\langle k_T \rangle$  in Fig. 6).

Suppression mechanisms may also exist at large  $p_T$  due to the restriction of phase space for gluon emission from large- $x$  partons. A gluon emitted from an incoming parton carries away a momentum fraction  $\Delta x = 2p_T e^y / \sqrt{s}$ , where  $y$  is the rapidity of the gluon. Since gluons emitted at forward rapidities would carry away more of the incident parton's momentum than available, the effective rapidity range for gluon emission becomes restricted to central rapidities. Such effects are not taken into account correctly in the simple  $k_T$  models discussed above.



Finally, there has been much recent interest in studying the effects of resumming large logarithms of the form  $\ln(1 - x_T)$ , where  $x_T = 2p_T/\sqrt{s}$  [34,35]. As  $x_T$  approaches 1, for any hard-scattering process, the perturbative cross section is enhanced by powers of  $\ln(1 - x_T)$  that have to be resummed at all orders. These types of effects should currently be negligible for direct-photon production at the Tevatron collider (because data are available only for relatively small values of  $x_T$ ), but may be important at fixed-target energies. Definitive answers to the question of whether this effect leads to a net enhancement or suppression, and its consequences for the shape of the  $p_T$  distribution, are not presently available. A treatment that includes both  $k_T$  and threshold resummation effects may be necessary for a more satisfactory description of the fixed-target data.

### Analytic Smearing Methods

An alternative to the Monte Carlo calculation of the  $k_T$  enhancement is its implementation through analytic convolution of the theoretical cross section with a (Gaussian)  $k_T$  distribution in either one or two dimensions. The latter is a better approximation, but the correction to the one-dimensional convolution is second order in  $k_T/p_T$ , leading to a difference of about 10% for the fixed-target applications. To compare to the Monte Carlo results, the parameters of such analytic convolutions must be interpreted in terms of the parton-level  $\langle k_T \rangle$  values.

We consider the kinematics of the production of a direct photon accompanied by a recoil jet. As mentioned before, the total transverse momentum imparted to the final state ( $\gamma$ +jet) by the colliding partons has an RMS width

$$\sigma_{2partons,2D} = \sqrt{2}\sigma_{1parton,2D}. \quad (9)$$

However, the single photon is subject only to half of this transverse kick, because it shares the total  $p_T$  with the recoil jet. Consequently, the  $k_T$  RMS width relevant for an analytic smearing of the single-inclusive photon cross section is

$$\sigma_{\gamma,2D} = \frac{1}{2}\sigma_{2parton,2D} = \frac{1}{\sqrt{2}}\sigma_{1parton,2D}. \quad (10)$$

The above can be illustrated by a simple example. Consider the production of a photon and a jet with equal and opposite  $p_T$  values (for example, 4 GeV/ $c$ ) close to 90 degrees in the center of mass. Compare this to the situation when the colliding partons impart some amount of  $k_T$ , say 1 GeV/ $c$ , in the direction of the photon. The photon  $p_T$  is now 4.5 GeV/ $c$ , and the jet  $p_T$  becomes 3.5 GeV/ $c$  (in the opposite direction), resulting from a total of 1 GeV/ $c$  of  $k_T$  imparted to the photon+jet system. Thus, the photon itself only receives half of the partonic total. This factor of two is critical, and can be easily overlooked, in calculating  $k_T$  smearing using analytic methods. The above conclusions have been verified within the explicit Monte Carlo treatment of event kinematics. (The convolution formulae for  $k_T$  smearing are discussed more fully in the Appendix.)

Recently, the MRST group has produced a new set of parton distributions, incorporating  $k_T$  effects in their analysis of the WA70 and E706 direct-photon data [36]; they used an analytic smearing technique rather than a Monte Carlo approach. The correction algorithm differs in detail with the one discussed above, and seems to require a significantly smaller  $\langle k_T \rangle$  to describe the data (about 0.65 GeV/ $c$  per incoming parton as compared to 1.2 GeV/ $c$  that was used for E706 at  $\sqrt{s} = 31.6$  GeV). This discrepancy may be due to a difference in the interpretation of  $k_T$  that is related to the factor of two present in Eq. 10. If we reinterpret the  $\langle k_T \rangle_{\text{MRST}}$  of 0.65 GeV/ $c$  as our 1.3 GeV/ $c$  per parton, then agreement is restored. Nevertheless, the  $k_T$ -enhancement factors differ somewhat in the two techniques, leading to different conclusions about the gluon distribution, especially at large  $x$  (see next section). For comparison, the MRST  $k_T$  factor for E706 (at  $\sqrt{s} = 31.6$  GeV) has also been plotted in Fig. 12; it is similar in size to our calculations for  $\langle k_T \rangle$  values in the range of 1.2–1.4 GeV/ $c$ , but has a different shape in  $p_T$ . Until these differences are understood, we must assume that there is a significant shape-dependent uncertainty associated with the particular assumptions used for modeling  $k_T$  effects.

## IMPACT ON THE GLUON DISTRIBUTION

It is now generally accepted that the uncertainty in the gluon distribution at large  $x$  is still quite large. Thus, it would appear important to incorporate further constraints on the gluon, especially from direct-photon data. In the following, we describe a global pdf fit that employs our  $k_T$  model in the analysis of E706 direct-photon measurements. Since jet production at the Tevatron collider is another available constraint for the gluon content at large  $x$ , we discuss the consistency between the E706 direct-photon results and the CTEQ4HJ gluon distribution (derived using high- $p_T$  jet data from CDF) [37].

### Application of $k_T$ Enhancements in a pdf Fit

To investigate the impact of  $k_T$  effects on determinations of the gluon distribution, we have included the E706 direct-photon cross sections for incident protons, along with the DIS and DY data that were used in determining the CTEQ4M pdfs, in a global fit to the parton distribution functions. The CTEQ fitting program was employed to obtain these results [38], using the NLO PQCD calculations for direct-photon cross sections, adjusted by the  $k_T$ -enhancement factors. However, the WA70, UA6, CDF, and DØ data were excluded from this particular fit. The resulting gluon distribution, shown in Fig. 13, is similar to CTEQ4M, as might have been expected, since the  $k_T$ -enhanced NLO cross sections using CTEQ4M provide a reasonable description of the data shown in Figs. 3 and 4.

The data sets used in determining CTEQ4M did not include the E706 direct-photon cross sections, but did use earlier direct-photon data from UA6 and from WA70 (without  $k_T$  corrections), along with the inclusive jet cross sections from CDF and DØ [39]. The jet cross sections were particularly useful for defining the gluon distribution in CTEQ4M at moderate values of  $x$ .

The new MRST gluon distribution (also shown in Fig. 13) is significantly lower than CTEQ4M (and MRSR2) at large  $x$ . While the MRST fit employs  $k_T$  enhancements, it

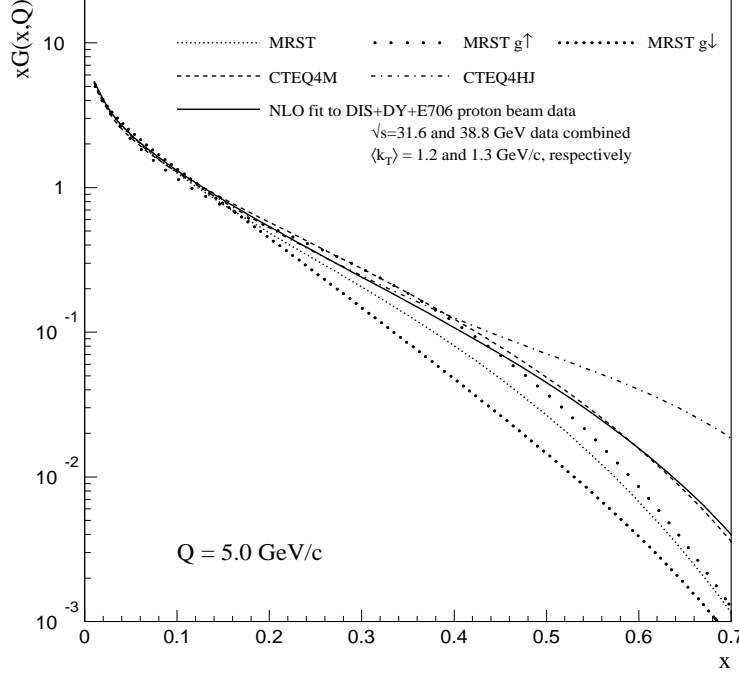


FIG. 13. A comparison of the CTEQ4M, MRST, and CTEQ4HJ gluons, and the gluon distribution derived from fits that use E706 data. The  $g\uparrow$  and  $g\downarrow$  gluon densities correspond to the maximum variation in  $\langle k_T \rangle$  that MRST allowed in their fits.

attempts to accommodate the WA70 incident-proton direct-photon data, which does not exhibit an obvious  $k_T$  effect. In addition, the MRST  $k_T$ -enhancement factors are larger at large  $p_T$  than our corresponding results, resulting in a smaller gluon at large  $x$ . This further serves to illustrate the extent to which the extracted gluon distribution is affected by the specific procedures applied in the fit. In contrast, the CTEQ4HJ specialized gluon distribution (discussed in more detail in the next subsection) is much larger than CTEQ4M in the same  $x$  range. The current spread of the solutions for the gluon distribution at large  $x$  is uncomfortably large, and additional effort is required to resolve these discrepancies.

## Discussion of the CTEQ4HJ Gluon

As presented above, when analyzed with  $k_T$ -enhancement factors, the E706 direct-photon data lead to a gluon distribution similar to that in CTEQ4M. The implications for the size of the gluon at large  $x$  are especially important because of the excess observed by CDF in the high- $p_T$  inclusive jet cross section (when compared to calculations using conventional pdfs). The CTEQ collaboration produced a global fit (CTEQ4HJ) [37] to improve the description of the high- $p_T$  jet data from CDF in Run IA [40]. The high- $p_T$  data points were given an enhanced weight to emphasize them in that fit. The resulting CTEQ4HJ parton distributions produce a jet cross section that by design follows the CDF data points more closely than the cross section obtained using CTEQ4M.

The CDF inclusive jet cross section from Run IB [42] demonstrates an excess at high  $p_T$  similar to that observed in Run IA. For DØ, the inclusive jet cross section from Run IA+IB is consistent with the NLO QCD calculation using conventional parton distributions such as CTEQ4M, but can also be well-described with calculations using the CTEQ4HJ parton distribution functions; in fact, calculations using CTEQ4HJ result in better  $\chi^2$  agreement with the DØ jet data [43].

The CTEQ4HJ quark distributions are similar to those obtained in a more standard fit (as for example CTEQ4M), since the DIS and DY data provide significant constraints on the quark distributions over all  $x$  (and on the gluon distribution at small  $x$ ) [3]. However, the CTEQ4HJ gluon distribution is significantly larger at high  $x$  than that of CTEQ4M, by a factor of 1.5 at  $x = 0.5$  (for  $Q = 5$  GeV/ $c$ ), and by a factor of 5 at  $x = 0.7$ .

Because of the dominance of the  $q\bar{q}$  scattering subprocess in the Tevatron jet cross sections at high  $p_T$ , a large change in the gluon distribution is required to generate a relatively small change in the jet cross section. As the CTEQ exercise has demonstrated, until the theoretical issues related to interpretation of direct-photon data are resolved, there is freedom within the data sets used in the global fits to change the gluon distribution in this way. It should also be noted that a recent analysis [41] of deuteron and proton structure functions, using corrections

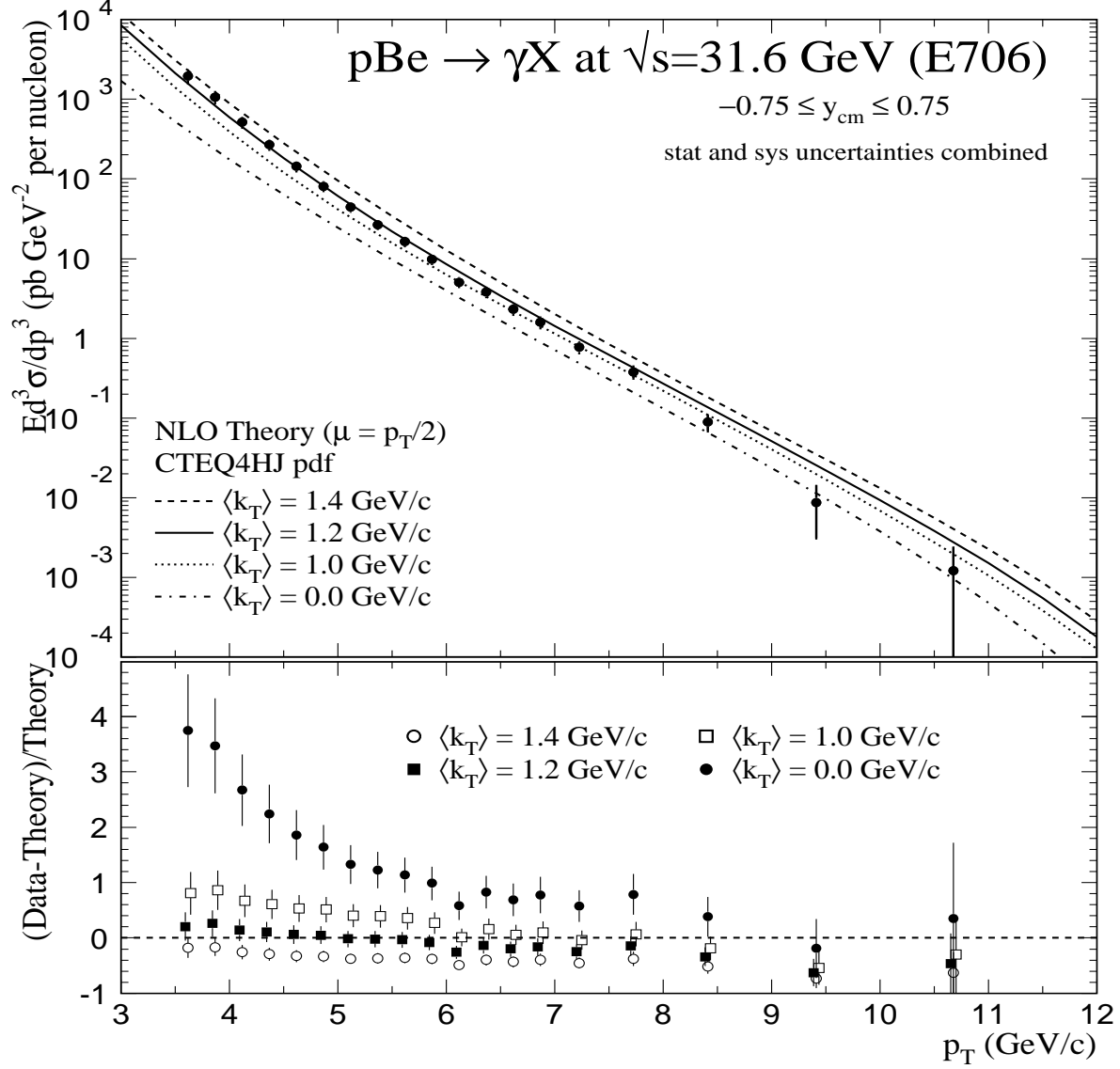


FIG. 14. Top: The photon cross section from E706 at  $\sqrt{s} = 31.6$  GeV compared to  $k_T$ -enhanced NLO calculations using the CTEQ4HJ parton distribution functions. Bottom: The quantity  $(\text{Data}-\text{Theory})/\text{Theory}$  using  $k_T$ -enhanced NLO calculations for several values of  $\langle k_T \rangle$ . The error bars have experimental statistical and systematic uncertainties added in quadrature.

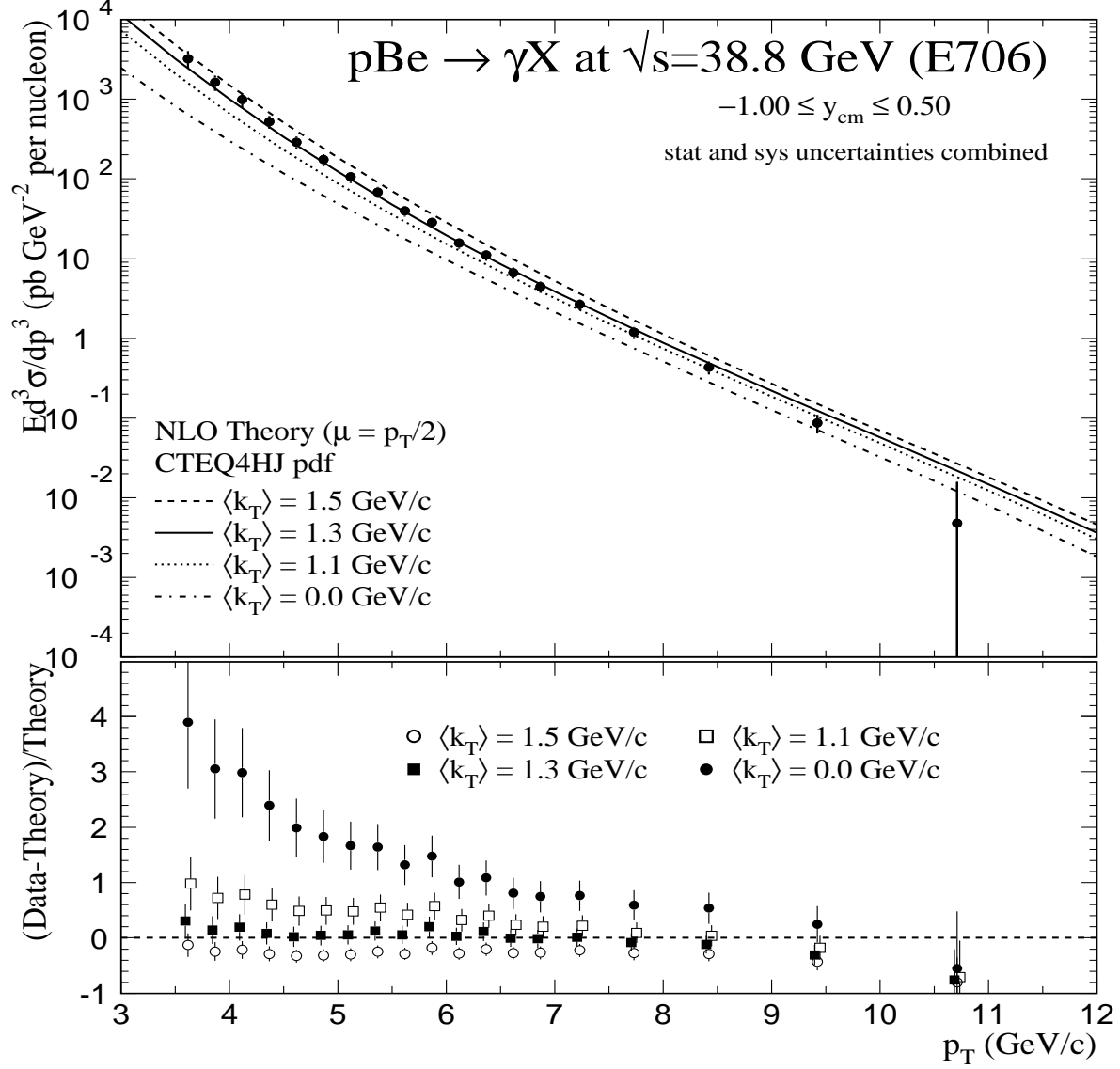


FIG. 15. Top: The photon cross section from E706 at  $\sqrt{s} = 38.8$  GeV compared to  $k_T$ -enhanced NLO calculations using the CTEQ4HJ parton distribution functions. Bottom: The quantity  $(\text{Data}-\text{Theory})/\text{Theory}$  using  $k_T$ -enhanced NLO calculations for several values of  $\langle k_T \rangle$ . The error bars have experimental statistical and systematic uncertainties added in quadrature.

for nuclear binding effects in the deuteron, suggests that the down-quark distribution in the nucleon at large  $x$  may be significantly larger than previously assumed; clearly this also influences the calculated cross sections for the high- $p_T$  jet production.

The CTEQ4HJ gluon distribution is compared to those from CTEQ4M, MRST, and the fits including the E706 data in Fig. 13. Figures 14 and 15 show comparisons of the E706 direct-photon cross sections and the NLO calculations using the CTEQ4HJ parton distributions, with and without the  $k_T$ -enhancement factor. The shape in  $p_T$  of these calculations appears less consistent with the data than the corresponding results using the CTEQ4M gluon. However, current uncertainties in the understanding of  $k_T$  effects in direct-photon production (discussed in the previous section), preclude an unambiguous interpretation of this difference.

## CONCLUSIONS

We have described a phenomenological model for  $k_T$  effects in which  $\langle k_T \rangle$  values used in the calculations of  $k_T$ -enhancement factors are derived from data. Despite uncertainties, the results are remarkably successful in reconciling the data and theoretical calculations for a broad range of energies. The  $k_T$ -enhancement factors improve the agreement of QCD calculations with E706, UA6, and  $\pi^-$  beam WA70 direct-photon cross sections over the full  $p_T$  range of measurements, and at the low- $p_T$  end of CDF and DØ results. All fixed-target  $\pi^0$  measurements also agree much better with such  $k_T$ -enhanced calculations.

The proper treatment of soft-gluon radiation in direct-photon cross sections can affect the extraction of the gluon distribution, especially at large values of  $x$ . In this particular treatment of  $k_T$  enhancement, the E706 data, which span the widest  $x$ -range of any direct-photon experiment, are in better agreement with the gluon distribution from CTEQ4M than from CTEQ4HJ. However, within the phenomenological approach, any physical mechanism which gives rise to less enhancement at large  $x$  than our specific model calculation can make the CTEQ4HJ gluon more consistent with the E706 data.



A definitive conclusion regarding the quantitative role of  $k_T$  effects in hard scattering, and reliable additional information on the large- $x$  gluon distribution, awaits more complete theoretical calculations. The new generation of direct-photon and inclusive jet measurements serves as a strong impetus, and provides a testing ground, for new theoretical developments, perhaps incorporating both  $k_T$  and large- $x$  resummation, which will have less model dependence than the formulations discussed in this paper. Further progress built on this interplay between theory and experiment will allow a more definitive determination of the gluon distribution, especially in the large- $x$  region, where significant uncertainties still remain.

### ACKNOWLEDGEMENTS

We thank S. Catani, S. Ellis, E. Kovacs, H.-L. Lai, M. Mangano, P. Nason, T. Sjöstrand, G. Snow, D. Soper, G. Sterman, J. Stirling, M. Werlen, and C.-P. Yuan for useful conversations.

- 
- [1] F. Halzen and D. Scott, *Phys. Rev.* **D21**, 1320 (1980).
  - [2] P. Aurenche *et al.*, *Phys. Lett.* **140B**, 87 (1984); *Nucl. Phys.* **B297**, 661 (1988).
  - [3] J. Huston *et al.*, hep-ph/9801444, submitted to *Phys. Rev.* **D**.
  - [4] A. Martin, W. Stirling, R. Roberts, *Phys. Lett.* **304B**, 155 (1995).
  - [5] H. L. Lai *et al.*, *Phys. Rev.* **D55**, 1280 (1997).
  - [6] P. Aurenche *et al.*, *Phys. Rev.* **D39**, 3275 (1989).
  - [7] M. Glück, E. Reya, A. Vogt, *Z. Phys.* **C67**, 433 (1995); *ibid.* **C53**, 127 (1992).
  - [8] J. Huston *et al.*, *Phys. Rev.* **D51**, 6139 (1995).

- [9] L. Apanasevich *et al.*, hep-ex/9711017, to be published in *Phys. Rev. Lett.*
- [10] G. Ballocci *et al.*, preprint CERN-EP/98-111, submitted to *Phys. Lett.*
- [11] M. Begel, Ph. D. thesis, University of Rochester, 1998, and references therein.
- [12] G. Altarelli, R. K. Ellis, M. Greco, G. Martinelli, *Nucl. Phys.* **B246**, 12 (1984).
- [13] C. Balázs, C.-P. Yuan, J.-W. Qiu, *Phys. Lett.* **B355**, 548 (1995).
- [14] C. Balázs and C.-P. Yuan, *Phys. Rev.* **D56**, 5558 (1997), and references therein.
- [15] P. Chiappetta, R. Fergani, J. Ph. Guillet, *Phys. Lett.* **B348**, 646 (1995).
- [16] C. Balázs, E. Berger, S. Mrenna, C.-P. Yuan, *Phys. Rev.* **D57**, 6934 (1998).
- [17] R. Feynman, R. Field, G. Fox, *Phys. Rev.* **D18**, 3320 (1978); A. P. Contogouris *et al.*, *Nucl. Phys.* **B179**, 461 (1981); *Phys. Rev.* **D32**, 1134 (1985).
- [18] G. Altarelli, hep-ph/9710434 (talk at Lepton-Photon '97); H. Montgomery, FERMILAB-CONF-97-193 (talk at DIS '97); M. Zieliński, *Nucl. Phys. (Proc. Suppl.)* **B64**, 84 (1998) (talk at QCD '97); J. Huston, plenary talk at the ICHEP conference in Vancouver, July 1998.
- [19] J. Collins and D. Soper, *Nucl. Phys.* **B193**, 381 (1981); *ibid.* **B213**, 545(E) (1983); *ibid.* **B197**, 446 (1982). J. Collins, D. Soper, G. Sterman, *Phys. Lett.* **B109**, 388 (1982); *ibid.* **B126**, 275 (1983); *Nucl. Phys.* **B223**, 381 (1983); *ibid.* **B250**, 199 (1985).
- [20] H.-L. Lai and H.-N. Li, hep-ph/9802414.
- [21] J. Owens, *Rev. Mod. Phys.* **59**, 465 (1987).
- [22] T. Sjöstrand, hep-ph/9508391.
- [23] F. Paige *et al.*, hep-ph/9804321.
- [24] G. Marchesini *et al.*, hep-ph/9607393.
- [25] See, e. g., S. Linn at the ICHEP conference in Vancouver, July 1998.

- [26] L. E. Gordon, *Nucl. Phys.* **B501**, 175 (1997).
- [27] S. Ellis, J. Huston, D. Soper, in preparation.
- [28] For E706, each QCD calculation has been adjusted by  $A^{\alpha-1}$  to account for nuclear dependence of production on a Be target ( $A = 9.01$ ), using  $\alpha = 1.04$  (1.08) for direct-photon ( $\pi^0$ ) data.
- [29] F. Aversa *et al.*, *Nucl. Phys.* **B237**, 105, (1989).
- [30] J. Binnewies, B. A. Kniehl, G. Kramer, *Phys. Rev.* **D52**, 4947 (1995).
- [31] M. Bonesini *et al.*, *Z. Phys.* **C38**, 371 (1988); *ibid.* **C37**, 535 (1988); *ibid.* **C37**, 39 (1987).
- [32] E. Bonvin *et al.*, *Phys. Lett.* **B236**, 523 (1990); *Z. Phys.* **C41**, 591 (1989).
- [33] See, e. g., W. J. Stirling and M. R. Whalley, *J. Phys. G.* **19** (1993) D1.
- [34] S. Catani, M. Mangano, P. Nason, hep-ph/9806484.
- [35] E. Laenen, G. Oderda, G. Sterman, hep-ph/9806467; N. Kidonakis, G. Oderda, G. Sterman, hep-ph/9803241; hep-ph/9801268.
- [36] A. Martin *et al.*, hep-ph/9803445; in their  $k_T$  algorithm, the MRST group smears the perturbative QCD distribution by first making an analytic continuation of  $(d\sigma/dp_T^2)_{\text{PQCD}}$  to small  $p_T$  ( $< 3$  GeV/c) and then convoluting with a Gaussian form  $(1/\pi\sigma)e^{-k_T^2/\sigma}$ , where  $\sigma = (4/\pi)\langle k_T \rangle_{\text{MRST}}^2$ .
- [37] J. Huston *et al.*, *Phys. Rev. Lett.* **77**, 444 (1996).
- [38] H.-L. Lai, Ph.D. thesis, Michigan State University, 1997.
- [39] F. Abe *et al.*, *Phys. Rev. Lett.* **77**, 438 (1996); D. Elvira, at Conference on DIS and Related Phenomena, Rome, April 1996.
- [40] F. Abe *et al.*, *Phys. Rev. Lett.* **77**, 438 (1996).
- [41] U. K. Yang and A. Bodek, hep-ph/9806458; U. K. Yang, A. Bodek, Q. Fan, hep-ph/9806457.

[42] See, e. g., A. Akopian at the Physics in Collision conference, Frascati, June 1998.

[43] See, e. g., J. Blazey at the ICHEP conference in Vancouver, July, 1998.

## Appendix

In this appendix, we collect formulae relevant to the analytic treatment of  $k_T$  effects in inclusive cross sections. As discussed in the main text, we assume a Gaussian description for the parton  $k_T$ -distributions; the width parameters entering the formulae are labeled explicitly to help keep track of their meaning.

For definiteness, let us consider direct-photon production. The full 2-dimensional convolution of the (parametrized) differential cross section  $\Sigma$  (for example,  $\Sigma = d\sigma/dp_T$ ) with the Gaussian  $k_T$ -smearing functions can be written as:

$$\begin{aligned} \Sigma'(p_T) = \int d^2k_{T_1} d^2k_{T_2} d^2q_T \frac{1}{\pi \langle k_{T_1}^2 \rangle} e^{-k_{T_1}^2 / \langle k_{T_1}^2 \rangle} \frac{1}{\pi \langle k_{T_2}^2 \rangle} e^{-k_{T_2}^2 / \langle k_{T_2}^2 \rangle} \\ \times \Sigma(q_T) \delta^{(2)}(\vec{p}_T - \vec{q}_T - \frac{1}{2}(\vec{k}_{T_1} + \vec{k}_{T_2})), \end{aligned} \quad (11)$$

or, integrating out the  $\delta$ -function constraints, as

$$\Sigma'(p_T) = \int d^2k_T \frac{1}{\pi \sigma_{\gamma,2D}^2} \exp(-k_T^2 / \sigma_{\gamma,2D}^2) \Sigma(|\vec{p}_T - \vec{k}_T|), \quad (12)$$

where  $\sigma_{\gamma,2D}$  is the width parameter appropriate for the smearing of the direct-photon inclusive distribution; it is related to the width of the parton  $k_T$ -distribution through Eq. (10).

The  $k_T$ -enhancement factors, defined as  $K(p_T) \equiv \Sigma'(p_T)/\Sigma(p_T)$ , can be calculated numerically. For a more intuitive treatment, one can simplify the discussion by reducing the above equation to a 1-dimensional case. Let us decompose the  $\vec{k}_T$  vector into components parallel and perpendicular to  $\vec{p}_T$ . Then only the parallel component strongly affects the value of the photon  $p_T$ , while the perpendicular component affects  $p_T$  much less for typical  $k_T \ll p_T$  configurations (since it adds to  $p_T$  in quadrature). Neglecting the effect of the perpendicular component, and integrating it out, one arrives at a 1-dimensional approximation:

$$\Sigma'(p_T) = \int_{-\infty}^{+\infty} dk_T \frac{1}{\sqrt{2\pi\sigma_{\gamma,1D}^2}} \exp(-k_T^2/2\sigma_{\gamma,1D}^2) \Sigma(p_T - k_T), \quad (13)$$

where

$$\sigma_{\gamma,1D} = \frac{1}{\sqrt{2}}\sigma_{\gamma,2D} = \frac{1}{2}\sigma_{1parton,2D}, \quad (14)$$

and we used Eq. (10) to relate  $\sigma_{\gamma,2D}$  and  $\sigma_{1parton,2D}$ .

Two particularly interesting special cases are the exponential form of the cross section, used to describe the data at fixed-target energies, and the  $1/p_T^n$  form, appropriate at colliders.

For an exponential representation of the cross section,  $\Sigma \sim \exp(-bp_T)$ , one obtains

$$K(p_T) = \exp\left(\frac{1}{8}b^2\sigma_{1parton,2D}^2\right) = \exp\left(\frac{1}{2\pi}b^2\langle k_T \rangle^2\right). \quad (15)$$

Using the LO calculation of  $pp \rightarrow \gamma X$  at  $\sqrt{s} = 31.6$  GeV (and  $\langle k_T \rangle = 0$ ), one finds  $b \approx 1.8 (\text{GeV}/c)^{-2}$  at  $p_T = 6.5$  GeV/ $c$  (a value in the middle of the  $p_T$  range of E706). The approximate 1-dimensional formula above yields  $K \approx 2.1$  for  $\langle k_T \rangle = 1.2$  GeV/ $c$ , compared to  $K^{\text{LO}} \approx 2.0$  obtained in the full LO Monte Carlo calculation. In general, despite the approximations in the treatment, the analytical results are quite close to the results of the LO calculations. The  $\frac{1}{\sqrt{2}}$  factor in the relation of  $\sigma_{\gamma,2D}$  and  $\sigma_{1parton,2D}$  (Eq. 10) is crucial to obtaining this consistency.

A different representation, useful, for example, for parametrizing CDF and DØ measurements, assumes  $\Sigma \sim 1/p_T^n$ . For this parametrization (or more general functional forms) one can expand  $\Sigma(p_T - k_T)$  as a power series in  $k_T$  (for  $k_T$  small compared to  $p_T$ ):

$$\Sigma(p_T - k_T) = \Sigma(p_T) + \frac{1}{2!}k_T^2\Sigma''(p_T) + \frac{1}{4!}k_T^4\Sigma^{(4)}(p_T) + \dots \quad (16)$$

(the odd powers of  $k_T$  integrate out to zero). One obtains:

$$K(p_T) = 1 + \frac{\langle k_T \rangle^2}{2\pi} \frac{n(n+1)}{p_T^2} + \frac{\langle k_T \rangle^4}{8\pi^2} \frac{n(n+1)(n+2)(n+3)}{p_T^4} + \dots \quad (17)$$

For a constant (or a slowly changing) slope parameter  $n$  (and for  $\langle k_T \rangle \ll p_T$ ), the effects of  $k_T$  smearing decrease as  $1/p_T^2$ , as might be expected for a power-suppressed process.